Supporting information

Electron-Deficient Diketone Unit Engineering for Non-fused Ring Acceptors Enabling Over 13% Efficiency in Organic Solar Cells

Dou Luo,[a] Lanqing Li,[b] Yongqiang Shi,[c] Kai Wang,[a] Jianqi Zhang,[d] Xugang Guo[b] and Aung Ko Ko Kyaw[a]*

Experimental Section

All manipulations involving air-sensitive reagents were performed under an inert atmosphere of dry nitrogen. Compounds 1,3-dibromo-5-(2-ethylhexyl)-4H-thieno[3,4-c]pyrrole-4,6(5H)-dione **(4)** [1], 2,8-dibromo-5-(2-ethylhexyl)-4H-dithieno[3,2-c:2',3'-e]azepine-4,6(5H)-dione **(5)** [2] were synthesized according to the method in the literature. All the other starting materials, unless otherwise specified, were purchased commercially and used as received without further purification.

Synthesis of 4,4-bis(2-ethylhexyl)-4H-cyclopenta[2,1-b:3,4-b']dithiophene **(1)**

4H-cyclopenta[2,1-b:3,4-b']dithiophene (3 g, 16.82 mmol), 2-ethylhexyl bromide (7.46 g, 38.68 mmol), KOH (2.8 g, 50.46 mmol), KI (8.37 g, 50.46 mmol) were added in 30 mL DMSO under nitrogen atmosphere and stirred at 0 ^{o}C for 10 min, then stirred at room temperature overnight. Then the mixture was poured into water and extracted with CH_2Cl_2 for three times. The organic layer was washed with water and then dried over $MgSO_4$. After removal of solvent, the crude product was purified on a silica-gel column chromatography using petroleum ether as the eluent to afford light yellow liquid (6.1 g, 90.1%). ^{1}H NMR (400 MHz, $CDCl_3$, ppm): δ 7.10 (d, J = 4.88 Hz, 2H), 6.93-6.91 (m, 2H), 1.92-1.81 (m, 4H), 1.06-0.80 (m, 18H), 0.75 (m, 6H), 0.59 (m, 6H). HRMS: calcd for $C_{25}H_{38}S_6$, 402.6; found, 402.5 (100%).

Synthesis of 4,4-bis(2-ethylhexyl)-4H-cyclopenta[2,1-b:3,4-b']dithiophene-2-carbaldehyde **(2)**

To a 100 mL two-necked flask, DMF (1 mL) and $POCl_3$ (0.82 mL, 8.92 mmol) were added in 30 mL 1,2-dichloroethane ($ClCH_2CH_2Cl$) at 0 °C under nitrogen atmosphere. After being stirred at 0 °C for 20 min, compound **1** (3 g, 7.44 mmol) was directly injected into the flask. Then the mixture was refluxed at 90 °C overnight. After being cooled to room temperature, NaOH aqueous solution was added and then the resulting mixture continued stirring for 20 min. Then the mixture was poured into water and extracted with CH_2Cl_2 for three times. The organic layer was washed with water and then dried over $MgSO_4$. After removal of solvent, the crude product was purified on a silica-gel column chromatography using petroleum ether as the eluent to afford a yellow oil (2.5 g, 78.1%). ^{1}H NMR (400 MHz, $CDCl_3$, ppm): δ 9.82 (s, 1H), 7.56 (t, *J* = 7.16 Hz, 1H), 7.37 (d, *J* = 4.92 Hz, 1H), 6.99 (m, 1H), 1.97-1.86 (m, 4H), 1.07-0.80 (m, 18H), 0.74 (t, *J* = 13.4 Hz, 6H), 0.61-0.56 (m, 6H). HRMS: calcd for $C_{26}H_{38}OS_2$, 430.7; found, 430.7 (100%).

Synthesis of 4,4-bis(2-ethylhexyl)-6-(tributylstannyl)-4H-cyclopenta[2,1-b:3,4-b']dithiophene-2-carbaldehyde **(3)**

To a 100 mL two-necked flask, compound **2** (2 g, 4.64 mmol) and dry THF (100 mL) were added under nitrogen atmosphere, and the solution was cooled to −78 °C. N-methylpiperazine (511.61 mg, 5.1 mmol) was then injected, followed by n-butyllithium (2.04 mL, 2.5M in hexane, 5.1 mmol), after which the reaction was stirred for 20 min. The reaction was then warmed to −20 °C, and the second addition of n-butyllithium (2.04 mL, 2.5M in hexane, 5.1 mmol) was then added dropwise in the solution and left stirring for another 30 min. Then, tributyltin chloride (1.56 g, 4.80 mmol) was added and stirred at −20 °C for 0.5 h. After that, the mixture was allowed to warm to room temperature and further stirred for 12 h. Finally, the mixture was poured into water and extracted with CH_2Cl_2. The organic layer was separated, dried over anhydrous $MgSO_4$. Removal of the solvents under reduced pressure yielded brown

oil (3.3 g, 97%). The crude product was used in the next step without further purification. ^{1}H NMR (400 MHz, $CDCl_3$, ppm): δ 9.79 (s, 1H), 7.53 (s, 1H), 6.97 (s, 1H), 1.91-1.88 (m, 4H), 1.66-1.49 (m, 2H), 1.34-1.30 (m, 18H), 1.13-1.07 (m, 4H), 0.96-0.87 (m,12H), 0.74-0.71 (m, 9H), 0.58-0.55 (m, 12H). HRMS: calcd for $C_{38}H_{64}OS_2Sn$, 719.7; found, 719.7 (100%).

Synthesis of 6,6'-(5-(2-ethylhexyl)-4,6-dioxo-5,6-dihydro-4H-thieno[3,4-c]pyrrole-1,3-diyl)bis(4,4-bis(2-ethylhexyl)-4H-cyclopenta[2,1-b:3,4-b']dithiophene-2-carbaldehyde) **(6)**

$Pd(PPh_3)_4$ (37.4 mg, 0.032 mmol) was added quickly to a mixture of compound **3** (782.4 mg, 1.08 mmol) and compound **4** (200 mg, 0.472 mmol) in toluene (30 mL) under nitrogen atmosphere. The reaction was heated at 110 °C for 24 h. After being cooled to room temperature, 50 mL of 2 mol/L KF solution was added and then the resulting mixture continued stirring for 20 min. After being filtered, the filtrate was treated with water and extracted with CH_2Cl_2. The organic layer was separated, dried over anhydrous $MgSO_4$ and concentrated under reduced pressure. The residue was subjected to column chromatography over silica gel using petroleum ether/CH_2Cl_2 as eluent to afford a dark red solid (344 mg, 65%). ^{1}H NMR (400 MHz, $CDCl_3$, ppm): δ 9.87 (s, 2H), 7.99-7.92 (m, 2H), 7.60 (t, J = 4 Hz, 2H), 3.61-3.60 (m, 2H), 2.03-1.95 (m, 7H), 1.40-1.25 (m, 12H), 0.99-0.90 (m, 34H), 0.77-0.71 (m, 12H), 0.64-0.60 (m, 18H). HRMS: calcd for $C_{66}H_{91}NO_4S_5$, 1122.75; found, 1122.71.

Synthesis of 6,6'-(5-(2-ethylhexyl)-4,6-dioxo-5,6-dihydro-4H-dithieno[3,2-c:2',3'-e]azepine-2,8-diyl)bis(4,4-bis(2-ethylhexyl)-4H-cyclopenta[2,1-b:3,4-b']dithiophene-2-carbaldehyde) **(7)**

$Pd(PPh_3)_4$ (31.48 mg, 0.027 mmol) was added quickly to a mixture of compound **3** (653.8 mg, 0.908 mmol) and compound **5** (200 mg, 0.395 mmol) in toluene (30 mL) under nitrogen atmosphere. The reaction was heated at 110 °C for 24 h. After being cooled to room temperature, 50 mL of 2 mol/L KF solution was added and then the resulting mixture continued stirring for 20 min. After being filtered, the filtrate was treated with water and extracted with

CH_2Cl_2. The organic layer was separated, dried over anhydrous $MgSO_4$ and concentrated under reduced pressure. The residue was subjected to column chromatography over silica gel using petroleum ether/CH_2Cl_2 as eluent to afford a dark red solid (285 mg, 60%). ^{1}H NMR (400 MHz, $CDCl_3$, ppm): δ 9.86 (s, 2H), 7.86 (t, *J* = 4 Hz, 2H), 7.58 (t, *J* = 4 Hz, 2H), 7.18 (t, *J* = 4 Hz, 2H), 4.34-4.22 (m, 2H), 2.01-0.85 (m, 10H), 1.38-1.28 (m, 9H), 1.00-0.88 (m, 34H), 0.77-0.73 (m, 12H), 0.66-0.61 (m, 18H). HRMS: calcd for $C_{70}H_{93}NO_4S_6$, 1204.87; found, 1204.85.

Synthesis of 2,2'-((2Z,2'Z)-(((5-(2-ethylhexyl)-4,6-dioxo-5,6-dihydro-4H-thieno[3,4-c]pyrrole-1,3-diyl)bis(4,4-bis(2-ethylhexyl)-4H-cyclopenta[2,1-b:3,4-b']dithiophene-6,2-diyl))bis(methanylylidene))bis(5,6-difluoro-3-oxo-2,3-dihydro-1H-indene-2,1-diylidene))dimalononitrile **(TPDC-4F)**

2-(5,6-difluoro-3-oxo-2,3-dihydro-1H-inden-1-ylidene)malononitrile (153.7 mg, 0.668 mmol) was added to a solution of compound **6** (250 mg, 0.222 mmol) in $CHCl_3$ (30 mL) under nitrogen atmosphere. Then 1 mL pyridine was injected into the solution. The mixture was stirred at 60 °C for 12 h. After being cooled to room temperature, the mixture was poured into water and extracted with CH_2Cl_2. The organic layer was washed with water and then dried over $MgSO_4$. After removal of solvent, the crude product was purified on a silica-gel column chromatography using CH_2Cl_2 as the eluent. **TPDC-4F** was obtained as a black solid (233 mg, 68%). ^{1}H NMR (400 MHz, $CDCl_3$, ppm): δ 8.91 (s, 2H), 8.56-8.52 (m, 2H), 8.13-8.06 (m, 2H), 7.72-7.68 (m, 4H), 3.64-3.62 (m, 2H), 2.08-1.95 (m, 9H), 1.43-1.32 (m, 10H), 1.01-0.90 (m, 34H), 0.76-0.61 (m, 30H). ^{13}C NMR (100 MHz, $CDCl_3$, ppm): δ 186.08, 165.56, 162.58, 160.49, 158.34, 156.40, 155.78, 153.16, 153.02, 140.02, 138.92, 138.14, 136.56, 136.14, 134.52, 130.03, 125.19, 125.02, 120.56, 114.85, 114.46, 112.54, 69.01, 54.41, 43.09, 38.29, 35.51, 34.30, 33.98, 30.54, 28.40, 27.58, 27.28, 23.89, 23.07, 22.82, 14.09, 10.58. HRMS: [M]

calcd for $C_{90}H_{95}F_4N_5O_4S_5$ 1547.07; found, 1547.4277. Anal. Calcd. for $C_{90}H_{95}F_4N_5O_4S_5$: C 69.87, H 6.19, N 4.53, S 10.36; found: C 69.89, H 6.20, N 4.39, S 10.30.

Synthesis of 2,2'-((2Z,2'Z)-(((5-(2-ethylhexyl)-4,6-dioxo-5,6-dihydro-4H-dithieno[3,2-c:2',3'-e]azepine-2,8-diyl)bis(4,4-bis(2-ethylhexyl)-4H-cyclopenta[2,1-b:3,4-b']dithiophene-6,2-diyl))bis(methanylylidene))bis(5,6-difluoro-3-oxo-2,3-dihydro-1H-indene-2,1-diylidene)) dimalononitrile **(BTIC-4F)**

2-(5,6-difluoro-3-oxo-2,3-dihydro-1H-inden-1-ylidene)malononitrile (85.9 mg, 0.373 mmol) was added to a solution of compound **7** (150 mg, 0.124 mmol) in $CHCl_3$ (30 mL) under nitrogen atmosphere. Then 1 mL pyridine was injected into the solution. The mixture was stirred at 60 °C for 12 h. After being cooled to room temperature, the mixture was poured into water and extracted with CH_2Cl_2. The organic layer was washed with water and then dried over $MgSO_4$. After removal of solvent, the crude product was purified on a silica-gel column chromatography using CH_2Cl_2 as the eluent. **BTIC-4F** was obtained as a black solid (148.1 mg, 70%). ^{1}H NMR (400 MHz, $CDCl_3$, ppm): δ 8.90 (s, 2H), 8.55-8.51 (m, 2H), 7.93-7.91 (s, 2H), 7.69-7.66 (t, *J* = 12 Hz, 4H), 7.24-7.22 (m, 2H), 4.34-4.22 (m, 2H), 2.05-1.94 (m, 9H), 1.42-1.26 (m, 10H), 1.03-0.89 (m, 34H), 0.77-0.63 (m, 30H). ^{13}C NMR (100 MHz, CDCl3, ppm): δ 186.01, 165.74, 161.28, 159.68, 158.24, 157.19, 155.74, 153.12, 142.26, 139.45, 138.20, 137.47, 136.51, 135.82, 135.40, 134.25, 129.92, 120.50, 119.94, 115.03, 114.81, 114.48, 112.58, 112.40, 68.54, 54.31, 49.34, 43.20, 37.88, 35.47, 34.07, 30.83, 28.73, 28.50, 27.35, 24.13, 23.15, 22.85, 14.14, 10.58. HRMS: [M] calcd for $C_{94}H_{97}F_4N_5O_4S_6$ 1629.19; found, 1629.4277. Anal. Calcd. for $C_{94}H_{97}F_4N_5O_4S_6$: C 69.30, H 6.00, N 4.30, S 11.81; found: C 69.55, H 5.91, N 4.11, S 11.59.

General Measurement and Characterization: ^{1}H NMR and ^{13}C NMR spectra was recorded on Bruker Ascend 400 MHz spectrometer, respectively. High-resolution mass spectra were obtained with Thermo Scientific^{TM} Q-Exactive. Elemental analyses (EAs) of compounds were performed on Vario EL cube with CHNS pattern in Fudan University (Shanghai, China). Thermogravimetric analysis (TGA) was performed on a Netzsch TG 209 at a heating rate of 10 °C min^{-1} under nitrogen atmosphere. Differential scanning calorimetry (DSC) measurements of **TPDC-4F** and **BTIC-4F** were performed on a Netzsch DSC 204 under nitrogen at a heating rate of 10 °C min^{-1}.

UV-Vis-NIR absorption spectra were recorded on a Shimadzu UV-3600 UV-Vis-NIR spectrometer. The PL spectra were measured by using a HORIBA LabRAM HR Evolution spectrometer and 583 and 785 nm as an excitation source. The neat PM6, **TPDC-4F, BTIC-4F** and PM6:**TPDC-4F**, PM6:**BTIC-4F** blend films were spin-cast on quartz glass from 10 mg mL^{-1} $CHCl_3$ solution (total concentration) at a speed of 2000 rpm.

Cyclic voltammetry (CV) was measured on a CHI630E Electrochemical Workstation equipped with a glass carbon working electrode, a platinum wire counter electrode, and an Ag/AgCl reference electrode. The measurements were carried out in dry dichloromethane with tetrabutylammonium hexafluorophosphate (0.1 mol L^{-1}) as the supporting electrolyte under a nitrogen atmosphere at a scan rate of 100 mV s^{-1}. The potential of Ag/AgCl reference electrode was internally calibrated by using the ferrocene/ferrocenium redox couple (Fc/Fc^{+}). Atomic force microscopy (AFM) measurements were carried out using a NanoMan VS microscope in the tapping mode. TEM images were obtained from a JEM-2100F instrument. The time-resolved PL (TRPL) measurements were performed with an Edinburgh Instruments

spectrometer (FLS980), the active layer film was excited by a 405 nm pulsed laser.

Fabrication of organic solar cells: All devices were fabricated based on conventional structure: ITO/PEDOT:PSS/active layer/PDINN/Ag. ITO-coated glass substrates were cleaned by sonification in acetone, detergent, deionized water, and isopropyl alcohol and dried in a nitrogen stream. The pre-cleaned ITO substrate was coated with PEDOT: PSS (filtered through a 0.45 μm PES filter) by spin-coating (4000 rpm. for 30 s, thickness of ~30 nm) and then baked at 150 °C on a hotplate for 15 min in air. The PEDOT:PSS-coated ITO substrates were transferred into a N_2-filled glove box for subsequent steps. The PM6:**TPDC-4F** and PM6:**BTIC-4F** (1:1.2 weight ratio) active layer prepared by spin-casting 1-chlorobenzene solution at 2000 rpm for 60 s. The total concentration was 20 mg mL^{-1} with 0.5% (v:v 99.5:0.5) 1-chloronaphthalene (CN) as the additive. The thickness is approximately 100 nm as measured by the profilometer. Before spin-coating the electron transporting layer, all active layers were thermally annealed at 120 °C for 10 min. Finally, 5 nm of the perylene diimide functionalized (PDINN)[3] (1 mg mL^{-1} in methanol) was spin-coated at 3000 rpm for 30 s on the active layer followed by the deposition of 100 nm Ag cathode under a under high vacuum (< 2×10^{-4} Pa). All the active devices area were 0.056 cm^2 through a shadow mask. The current density–voltage (*J–V*) curves were measured using Keithley 2400 source meter under 1 sun (AM 1.5 G spectrum) generated from a class solar simulator (Japan, SAN-EI, XES-40S1). The external quantum efficiency (EQE) spectra were measured using a Solar Cell Spectral Response Measurement System QE-R3011 (Enlitech Co., Ltd.). The light intensity at each wavelength was calibrated using a standard single crystal Si photovoltaic cell.

Fabrication of single-carrier devices: Single-carrier device (ITO/PEDOT:PSS(40

nm)/active layer/MoO_3(10 nm)/Ag) and (ITO/ZnO(40 nm)/[4]active layer/PDINN/Ag) were fabricated to measure hole and electron mobility of the PM6:**TPDC-4F**, PM6:**BTIC-4F** blend films. The active layers comprising PM6:**TPDC-4F**, PM6:**BTIC-4F** were spin-cast from 1-chlorobenzene solution at 2000 rpm for 60 s (total concentration, 20 mg mL^{-1}). The thickness is approximately 100 nm as measured by the profilometer. The as-cast pure films of **TPDC-4F** and **BTIC-4F** were spin-cast from 1-chlorobenzene solution (total concentration, 15 mg mL^{-1}) at 1200 rpm for 60 s. The thickness is approximately 100 nm.

The mobility μ was derived from the SCLC model which is described by the equation $J = (9/8)\varepsilon_0\varepsilon_r\mu(V^2/d^3)$,[5] where J is the current, ε_0 the permittivity of free space, ε_r the relative permittivity of the material, d the thickness of the active layers, and V the effective voltage.

Table S1. Photovoltaic parameters of OSCs based on PM6:**TPDC-4F** blended films with different D:A ratio under the illumination of AM 1.5 G, 100 mW cm^{-2}.

Active layer	wt/wt	V_{oc} (V)	J_{sc} (mA cm^{-2})	*FF* (%)	PCE (%)
PM6**:TPDC-4F**	1:1	0.87	18.79	55.48	9.06
	1:1.2	0.872	20.86	56.12	10.20
	1:1.5	0.859	19.94	56.53	9.68

Table S2. Photovoltaic parameters of OSCs based on PM6:**TPDC-4F** (D:A=1:1.2, wt/wt) blended films with different thermal annealing temperature, annealing time and amount of 1-chloronaphthalene (CN) under the illumination of AM 1.5 G, 100 mW cm^{-2}.

Active layer	TA	Additive	V_{oc} (V)	J_{sc} (mA cm^{-2})	*FF* (%)	PCE (%)
PM6:**TPDC-4F** (1:1.2)	110 °C + 10 min	/	0.859	21.03	68.16	12.31
	120 °C + 10 min	/	0.859	21.10	69.13	12.52
	130 °C + 10 min	/	0.849	19.16	67.39	10.96
	120 °C + 5 min	/	0.859	21.07	68.90	12.47
	120 °C + 10 min	/	0.859	21.10	69.13	12.52
	120 °C + 20 min	/	0.85	20.32	66.69	11.51
	120 °C + 10 min	0.25% CN	0.853	22.13	69.7	13.15
	120 °C + 10 min	0.5% CN	0.852	22.19	70.6	13.35
	120 °C + 10 min	0.75% CN	0.84	22.05	70.1	12.98

Table S3. Photovoltaic parameters of OSCs based on PM6:**BTIC-4F** blended films with different D:A ratio under the illumination of AM 1.5 G, 100 mW cm^{-2}.

Active layer	wt/wt	V_{oc} (V)	J_{sc} (mA cm^{-2})	*FF* (%)	PCE (%)
PM6**:BTIC-4F**	1:1	0.91	17.65	45.8	7.35
	1:1.2	0.91	18.98	46.82	8.08
	1:1.5	0.90	18.3	44.5	7.32

Table S4. Photovoltaic parameters of OSCs based on PM6:**BTIC-4F** (D:A=1:1.2, wt/wt) blended films with different thermal annealing temperature, annealing time and amount of 1-chloronaphthalene (CN) under the illumination of AM 1.5 G, 100 mW cm^{-2}.

Active layer	TA	Additive	V_{oc} (V)	J_{sc} (mA cm^{-2})	*FF* (%)	PCE (%)
PM6:**BTIC-4F** (1:1.2)	110 °C + 10 min	/	0.9	19.20	57.88	10.0
	120 °C + 10 min	/	0.897	19.81	61.09	10.85
	130 °C + 10 min	/	0.897	18.7	59.29	9.94
	120 °C + 5 min	/	0.899	19.50	59.54	10.43
	120 °C + 10 min	/	0.897	19.81	61.09	10.85
	120 °C + 20 min	/	0.89	18.72	60.16	10.02
	120 °C + 10 min	0.25% CN	0.896	19.7	64.3	11.32
	120 °C + 10 min	0.5% CN	0.894	20.5	65.7	12.04
	120 °C + 10 min	0.75% CN	0.89	20.1	65.1	11.64

Table S5. Hole and electron mobility in single-carrier devices for pure **TPDC-4F**, **BTIC-4F** film and for the PM6:**TPDC-4F**, PM6:**BTIC-4F** blend films.

Blends film	μ_h ($cm^2\ V^{-1}\ s^{-1}$)	μ_e ($cm^2\ V^{-1}\ s^{-1}$)	μ_h / μ_e ratio
TPDC-4F	–	8.00×10^{-4}	–
BTIC-4F	–	6.63×10^{-4}	–
PM6:**TPDC-4F**	4.11×10^{-4}	4.06×10^{-4}	1.01
PM6:**BTIC-4F**	3.60×10^{-4}	2.78×10^{-4}	1.29

Table S6. Morphology data of PM6, **TPDC-4F** and **BTIC-4F** neat films and corresponding blended films.

	in plane (IP)				out of plane (OOP)			
Film	Position ($Å^{-1}$)	D-spacing[a] Å	FWHM Å	CCL[b] Å	Position ($Å^{-1}$)	D-spacing[a] Å	FWHM Å	CCL[b] Å
PM6	0.289	21.73	0.083	67.94	1.68	3.71	0.366	15.43
TPDC-4F	0.392	16.02	0.189	29.84	1.73	3.60	0.348	16.20
BTIC-4F	1.754	3.58	0.349	16.19	0.39	15.74	0.278	20.26
PM6:**TPDC-4F**	0.297	21.14	0.051	109.74	1.73	3.61	0.316	17.88
PM6:**BTIC-4F**	0.298	21.04	0.058	96.71	1.72	3.64	0.348	16.23

[a] Obtained using the equation of $d = 2\pi/q$, in which q is the corresponding x-coordinate of the diffraction peak. [b] Calculated using the equation: $CCL = 2\pi K/w$, in which w is the full width at half maxima and K is a form factor.

Table S7. The representative device performance reported in the literatures for non-fused core electron acceptors.

Active layer	V_{oc} (V)	J_{sc} (mA cm^{-2})	*FF* (%)	PCE (%)	Ref.
PBDB-T:**DF-PCIC**	0.91	15.66	72.1	10.14	[6]
PBDB-T:**DF-PCNC**	0.86	18.16	72.6	11.63	[7]
PBDB-TF:**HF-PCIC**	0.91	11.78	70.7	11.49	[8]
PBDB-TF:**HFO-PCIC**	0.93	12.62	70.99	8.36	[8]
PBDB-TF:**OF-PCIC**	0.91	13.76	73.37	9.09	[8]
PBDB-TF:**HF-TCIC**	0.76	20.04	65	9.86	[9]
PBDB-TF:**DF-TCIC**	0.86	16.39	58	8.23	[9]
PBDB-T:**FO-PCIC**	0.90	15.02	61.12	8.32	[10]
PBDB-TF:**HC-PCIC**	0.89	18.13	72.1	11.75	[10]
PBDB-T:**X-PCIC**	0.84	21.8	62.5	11.5	[11]
PBDB-T:**X1-PCIC**	0.85	17.97	68.82	10.17	[11]
PBDB-T-2Cl:**BTCIC-4Cl**	0.75	21.0	66	10.5	[12]
PBDB-T:**BDTS-4Cl**	0.83	9.8	45.9	3.73	[13]
PBDB-T:**BDTC-4Cl**	0.86	18.56	59.5	9.54	[13]
PBDB-T:**BTOR-IC-4F**	0.8	20.57	69.6	11.48	[14]
PBDB-T:**BCDT-4F**	0.80	18.28	66	9.65	[15]
PBDB-T:**BCDT-4Cl**	0.76	23.77	67	12.10	[15]
PBDB-T:**TPDCIC**	0.83	18.16	67.1	10.12	[16]
PBDB-T:**TPDCNC**	0.80	17.4	70.4	9.80	[16]
PM7: **BT2FIDT-4Cl**	0.97	18.1	71.5	12.5	[17]
PM7: **BO2FIDT-4Cl**	0.96	16.1	61.3	10.4	[17]
PBDB-T:**DOC2C6-2F**	0.85	21.35	73.1	13.24	[18]
J52:**UF-EH-2F**	0.79	24.87	69	13.56	[19]
PBDB-T:**BTzO-4F**	0.83	23.58	69.73	13.8	[20]

PM6:**BDC-4F-C8**	0.895	21.32	65.71	12.53	[21]
PTB7-Th:**SiOTIC-4F**	0.65	21.6	61.4	9.0	[22]
PTB7-Th:**COTIC-4F**	0.56	20.3	56.3	7.4	[22]
PTB7-Th:**CTIC-4F**	0.70	23.4	64	10.5	[23]
PTB7-Th:**CO1-4F**	0.64	24.8	64	10.2	[23]
PBDB-T:**PTIC**	0.93	16.73	66	10.27	[24]
PBDB-T:**CPDT-4F**	0.68	20.1	69.6	9.47	[25]
PBDB-T:**ITDI**	0.94	13.94	59.78	8.0	[26]
PTB7:**DTDfBT(TDPP)$_2$**	0.81	12.10	51	5.0	[27]
P:**DPP8**	0.90	13.78	58	7.19	[28]
P:**MPU1**	0.98	12.37	62	7.52	[29]
DTS(QxHTh2)2:**MPU2**	0.94	12.15	68	7.76	[30]
SMD:**MPU3**	0.98	13.72	67	9.14	[31]
J52:**BN-2F**	0.81	25.25	70.78	14.53	[32]
PBDB-T:**PCBM-C10**	0.87	21.30	72.66	13.55	[33]
PBDB-T:**TPDC-4F**	0.852	22.19	70.6	13.35	***This work***
PBDB-T:**BTIC-4F**	0.894	20.5	65.7	12.04	***This work***

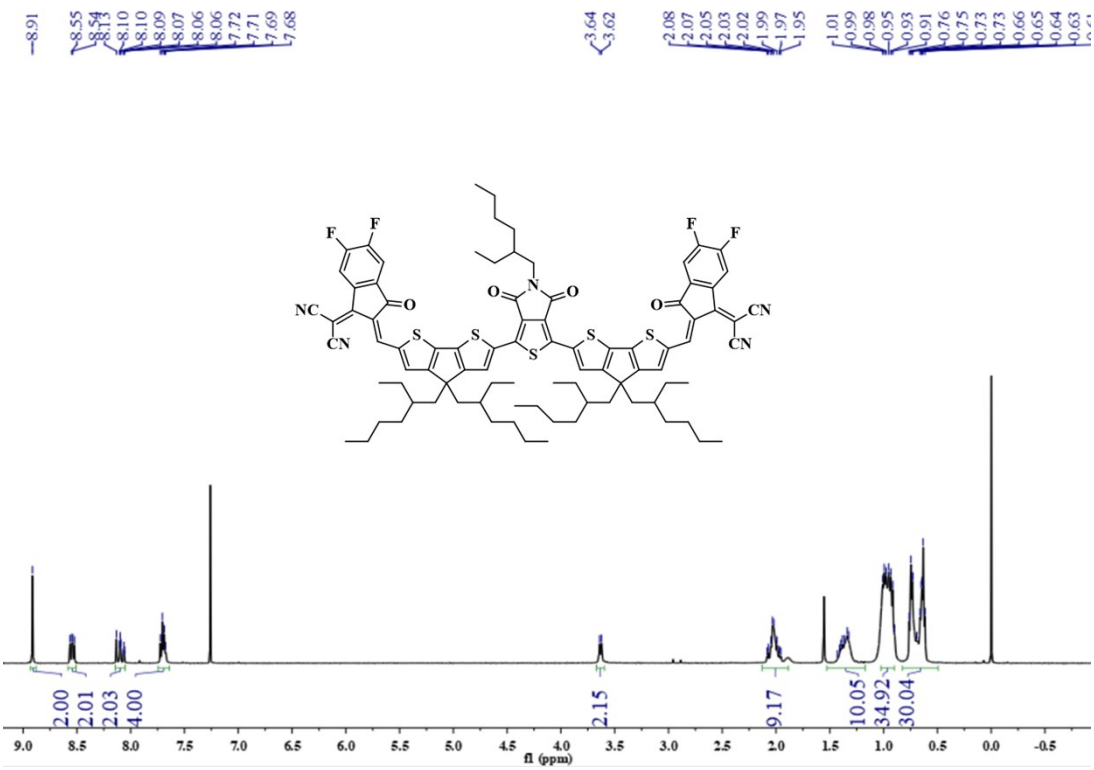

Fig. S1 ^{1}H NMR spectrum of **TPDC-4F** ($CDCl_3$, 400 MHz).

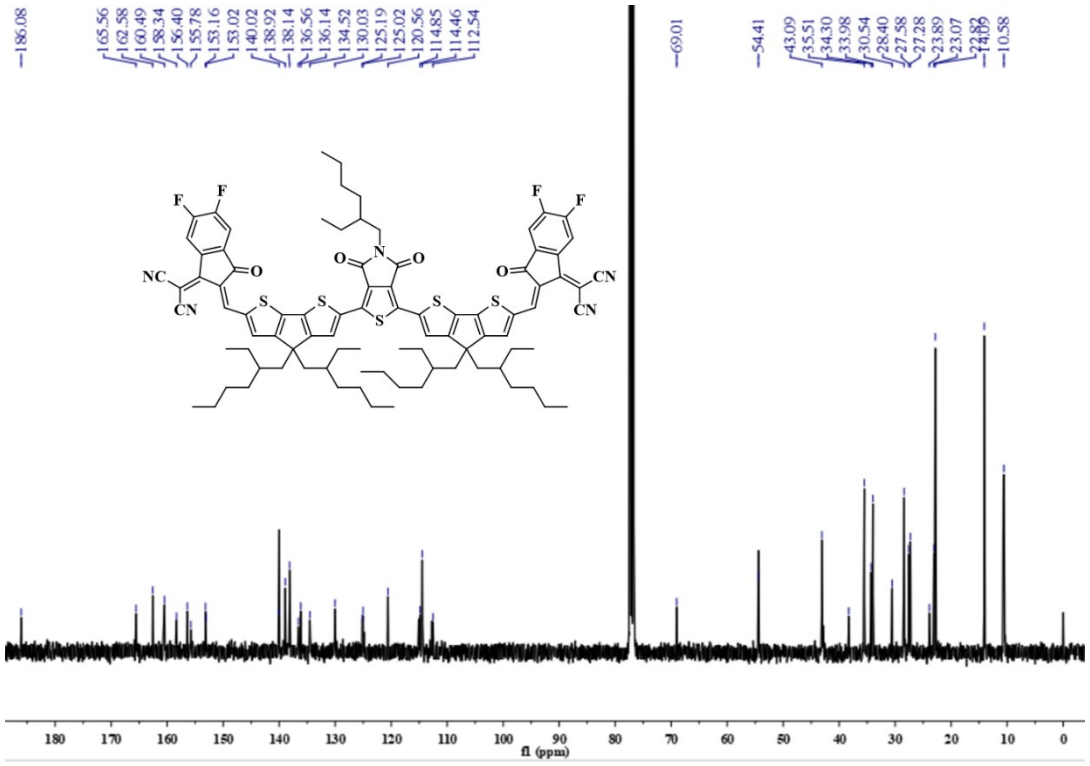

Fig. S2 ^{13}C NMR spectrum of **TPDC-4F** ($CDCl_3$, 400 MHz).

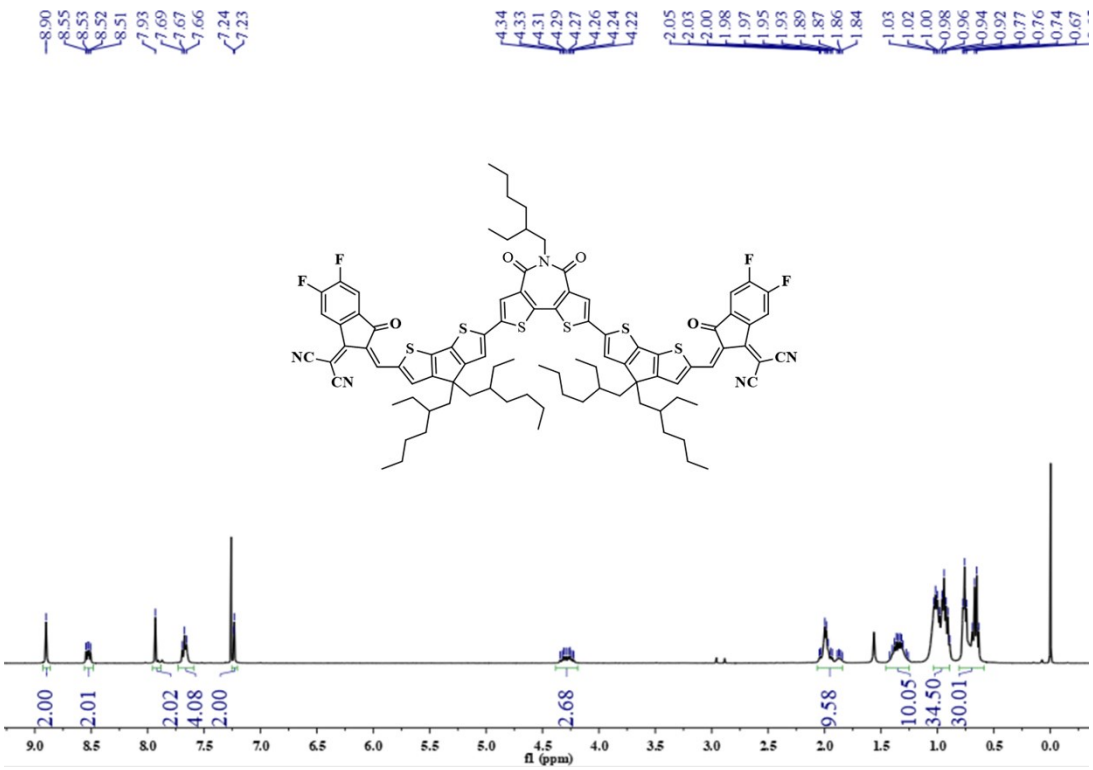

Fig. S3 ^{1}H NMR spectrum of **BTIC-4F** ($CDCl_3$, 400 MHz).

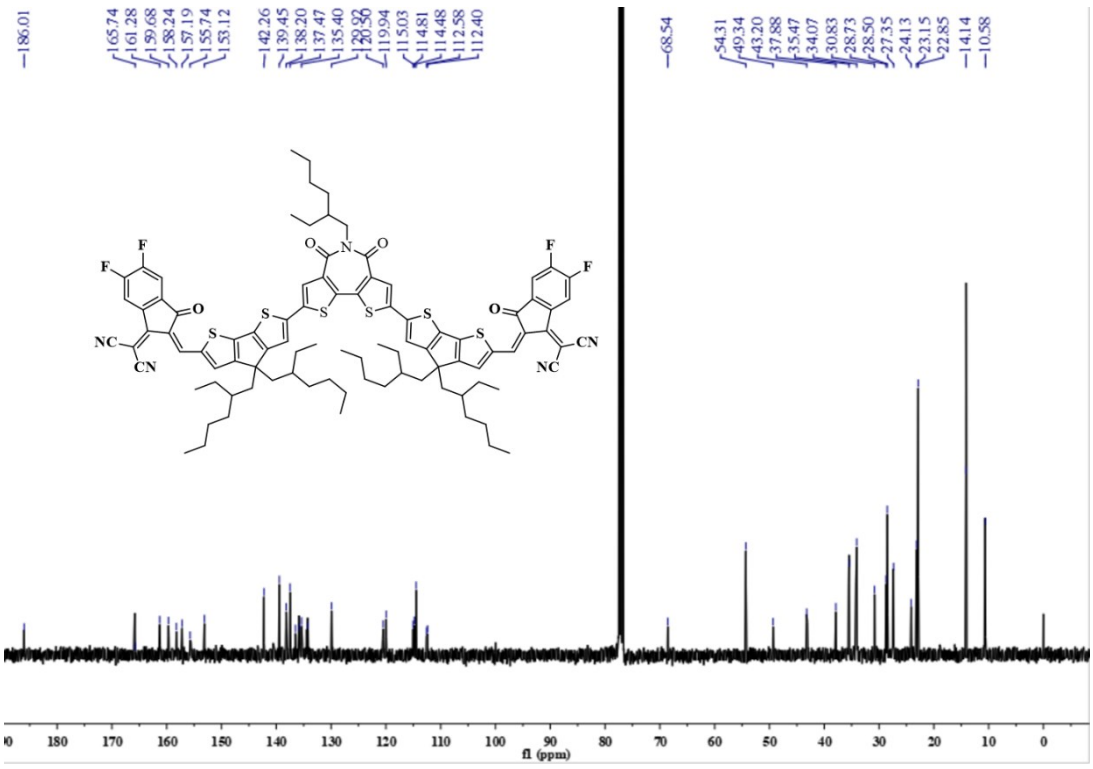

Fig. S4 ^{13}C NMR spectrum of **BTIC-4F** ($CDCl_3$, 400 MHz).

Positive:

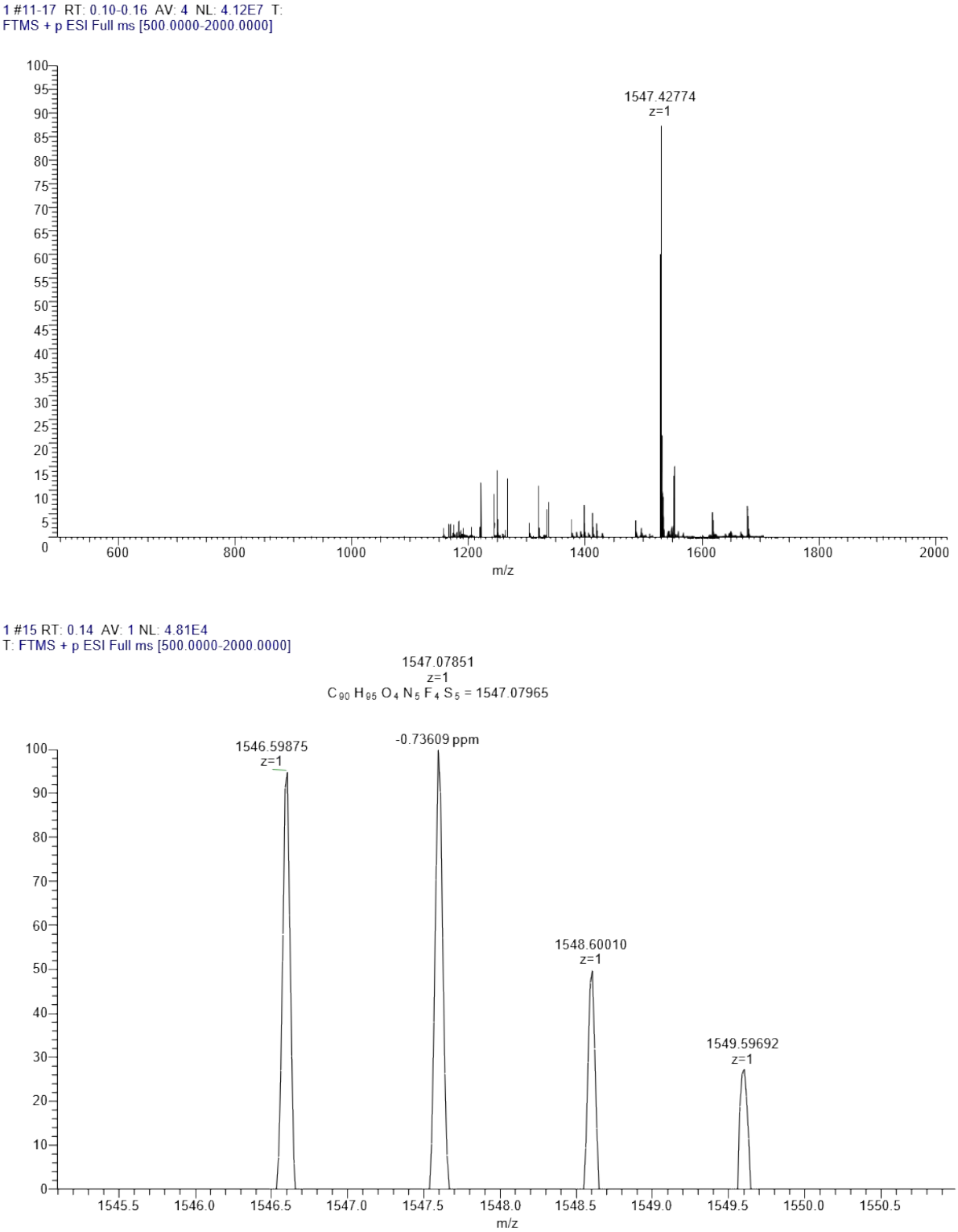

Fig. S5 HRMS of **TPDC-4F**.

Positive:

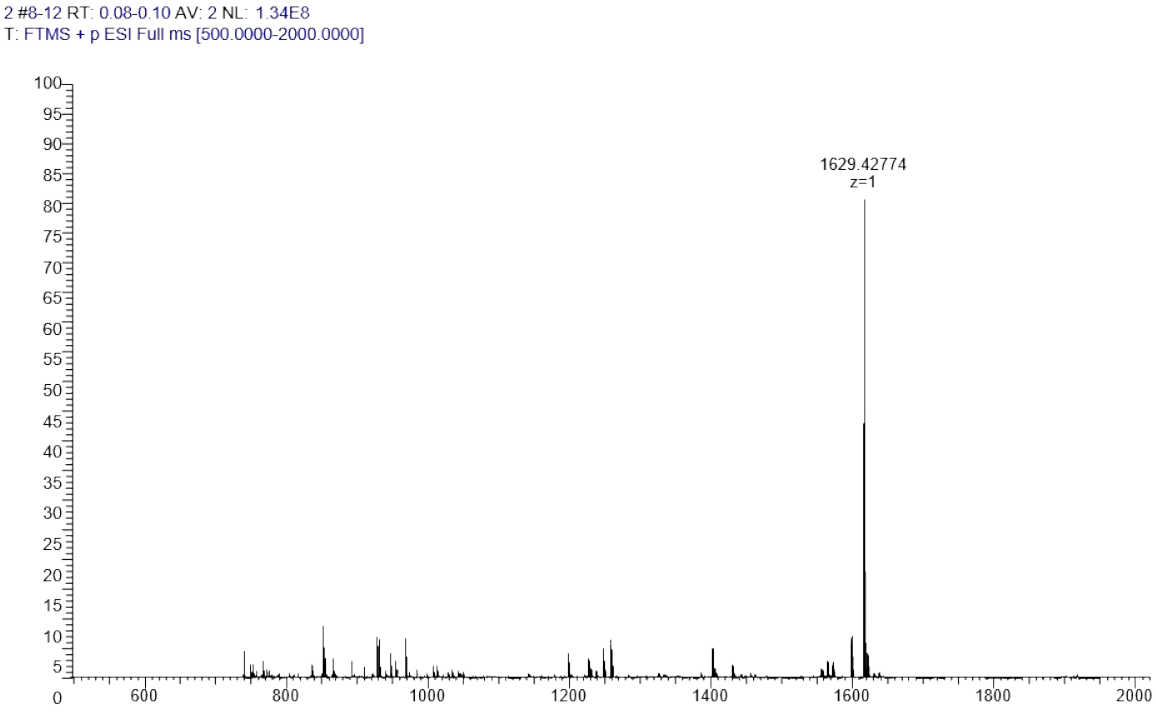

$[C_{94}H_{97}F_4N_5O_4S_6+H]^+$

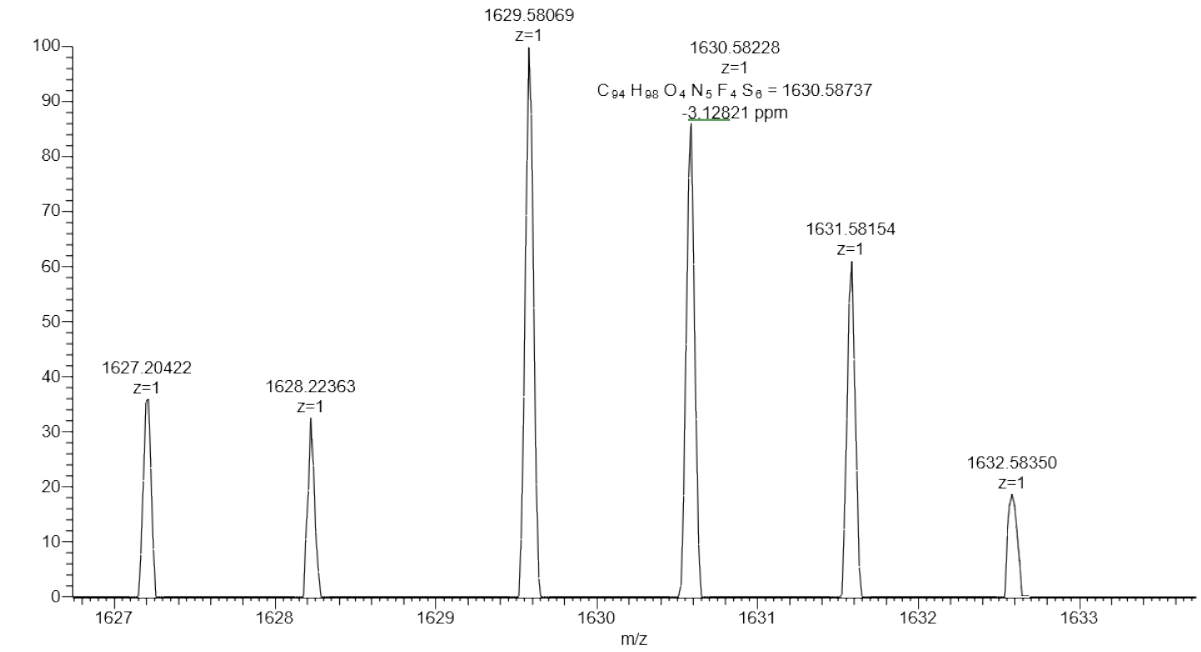

Fig. S6 HRMS of **BTIC-4F**.

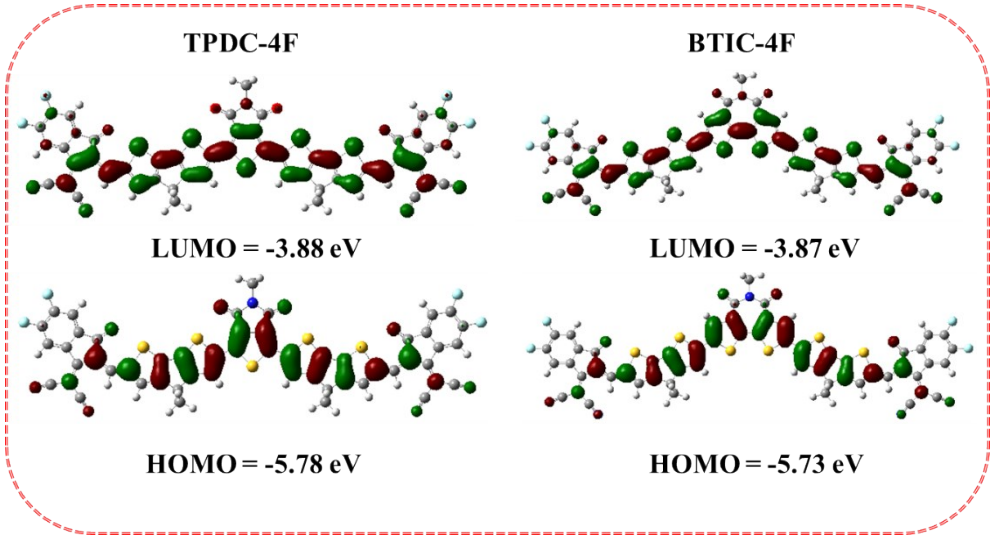

Fig. S7 Spatial structure models and HOMO/LUMO levels of **TPDC-4F** and **BTIC-4F** calculated by Gaussian 09 with density function theory (DFT) at the level of B3LYP/6-31G. The alkyl chains were replaced with methyl groups.

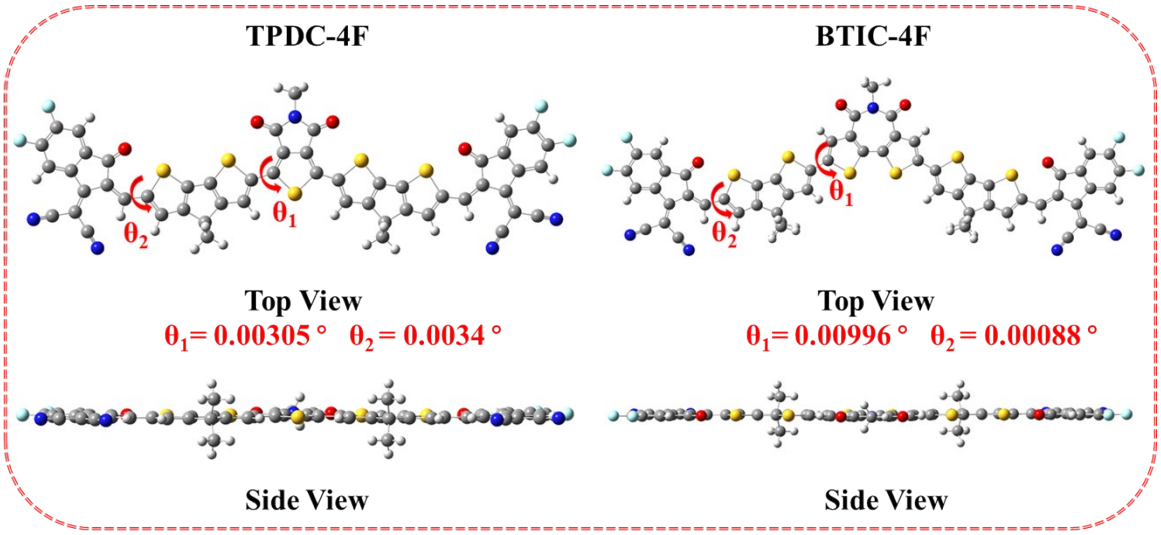

Fig. S8 Representative dihedral angles of **TPDC-4F** and **BTIC-4F** calculated by Gaussian 09 with density function theory (DFT) at the level of B3LYP/6-31G. The alkyl chains were replaced with methyl groups.

Acceptor	Chlorobenzene (16 mg/mL in CB)	Chloroform (20 mg/mL in CF)
TPDC-4F		
		
BTIC-4F		
		

Fig. S9 The solubilities of **TPDC-4F** and **BTIC-4F** in chlorobenzene and chloroform solution at room temperature.

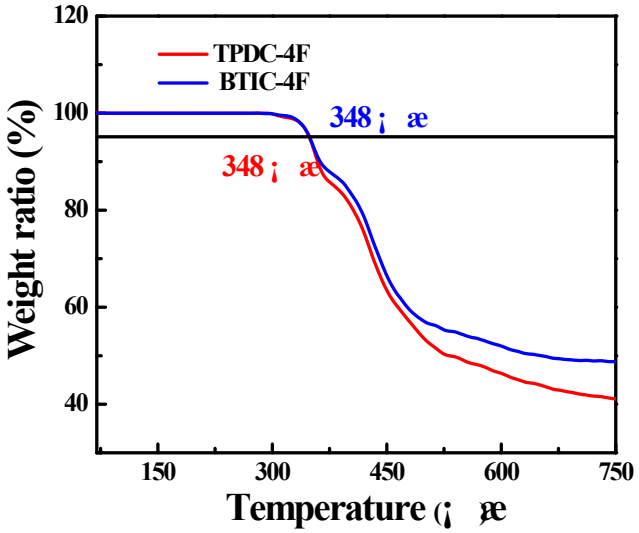

Fig. S10 TGA diagrams of **TPDC-4F** and **BTIC-4F.**

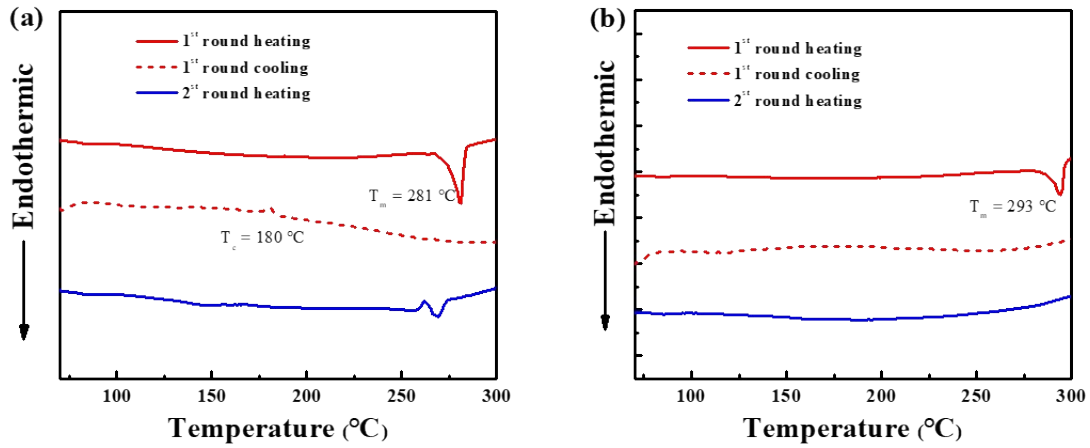

Fig. S11 DSC diagrams of **TPDC-4F** (a) and **BTIC-4F** (b)**.**

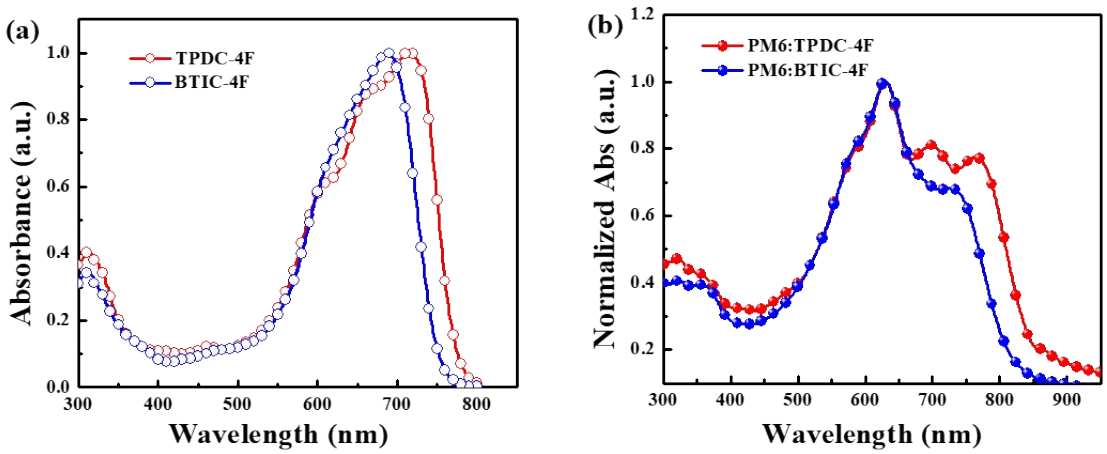

Fig. S12 Normalized UV-vis absorption spectra of (a) **TPDC-4F** and **BTIC-4F** in solution (b) PM6:**TPDC-4F** and PM6:**BTIC-4F** blend film.

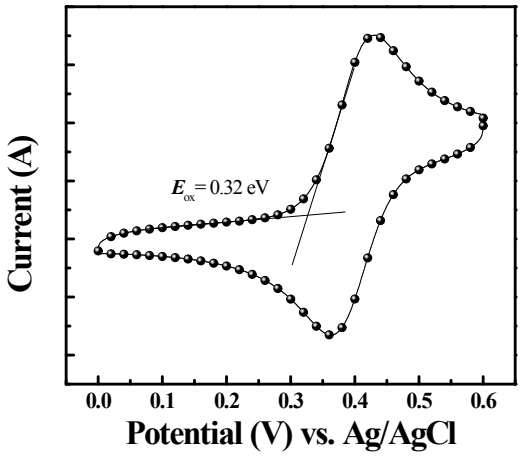

Fig. S13 Cyclovoltammetry curves of ferrocene.

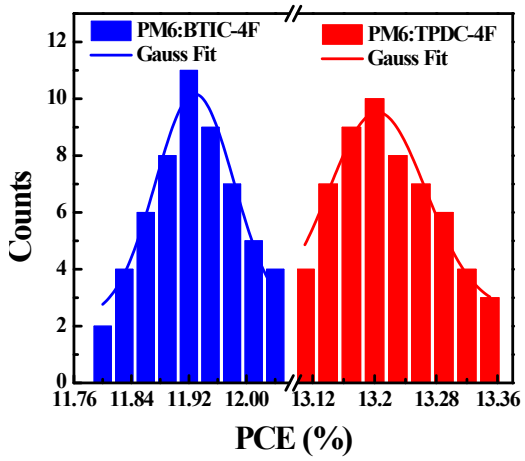

Fig. S14 Histogram of PM6:**TPDC-4F** and PM6:**BTIC-4F** solar cell efficiencies for 64 and 56 devices, respectively.

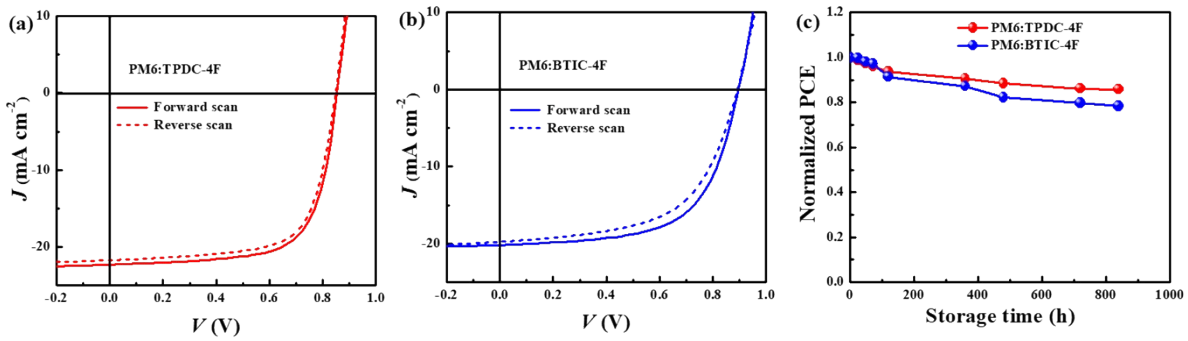

Fig. S15 *J*–*V* curves of (a) PM6:**TPDC-4F** and (b) PM6:**BTIC-4F** in different scan directions. (c) The stability of **TPDC-4F**- and **BTIC-4F**-based devices in a N_2-filled glovebox without encapsulation.

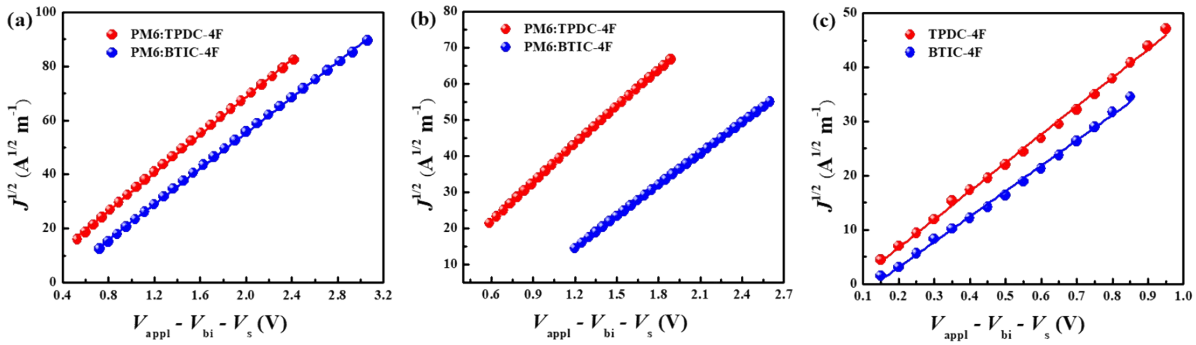

Fig. S16 The $J^{1/2}$–V characteristics of the hole-only (a) and electron-only (b) devices based on the blend films PM6:**TPDC-4F** and PM6:**BTIC-4F**, and (c) The $J^{1/2}$–V characteristic of the electron-only device based on the pure film of **TPDC-4F** and **BTIC-4F**.

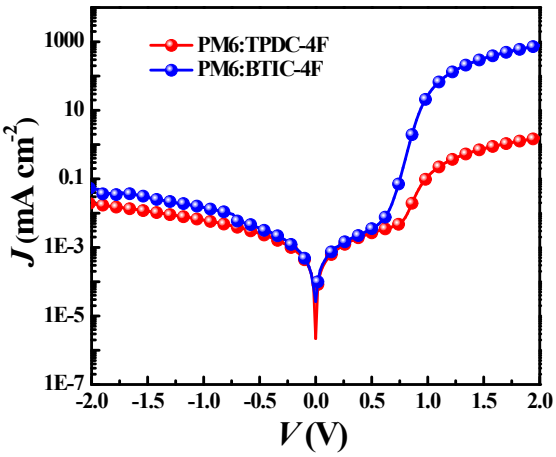

Fig. S17 Dark J–V characteristics of the photovoltaic devices of PM6:**TPDC-4F** and PM6:**BTIC-4F**.

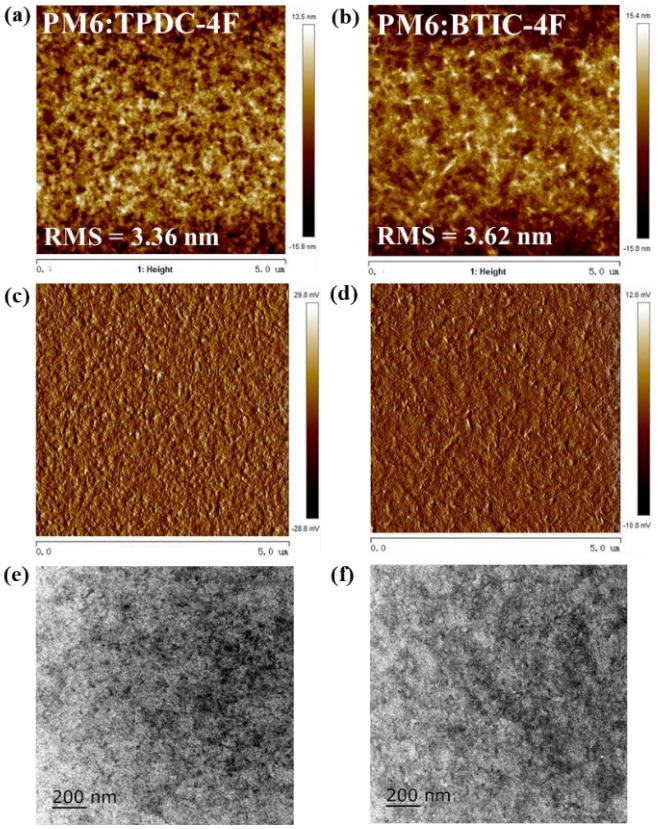

Fig. S18 Tapping-mode AFM height images of (a) PM6:**TPDC-4F**, (b) PM6:**BTIC-4F** blend films and the corresponding phase images of (c) PM6:**TPDC-4F**, (d) PM6:**BTIC-4F** blend films. TEM images of (e) PM6:**TPDC-4F** and (f) PM6:**BTIC-4F** blend films. Scale bar: 200 nm

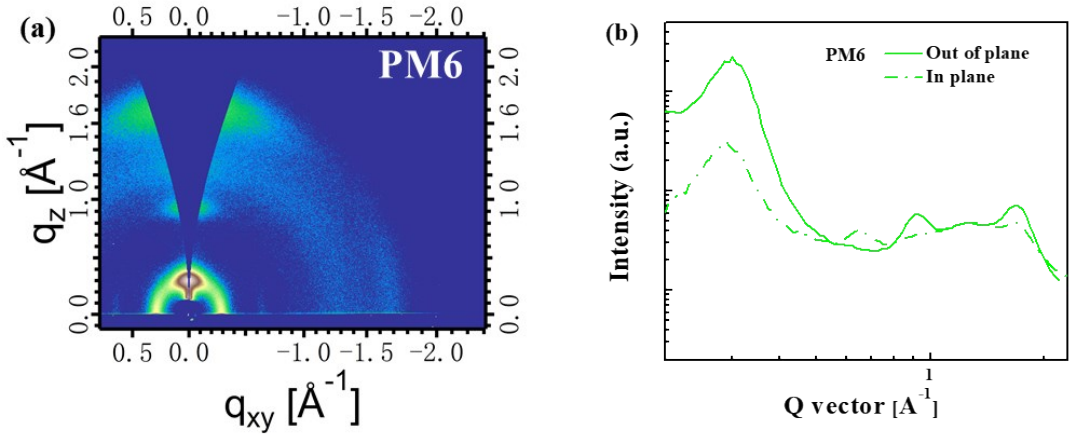

Fig. S19 (a) GIWAXS patterns of PM6 neat film. (b) out-of-plane (solid line) and in-plane (dotted line) line-cut profiles of PM6 film.

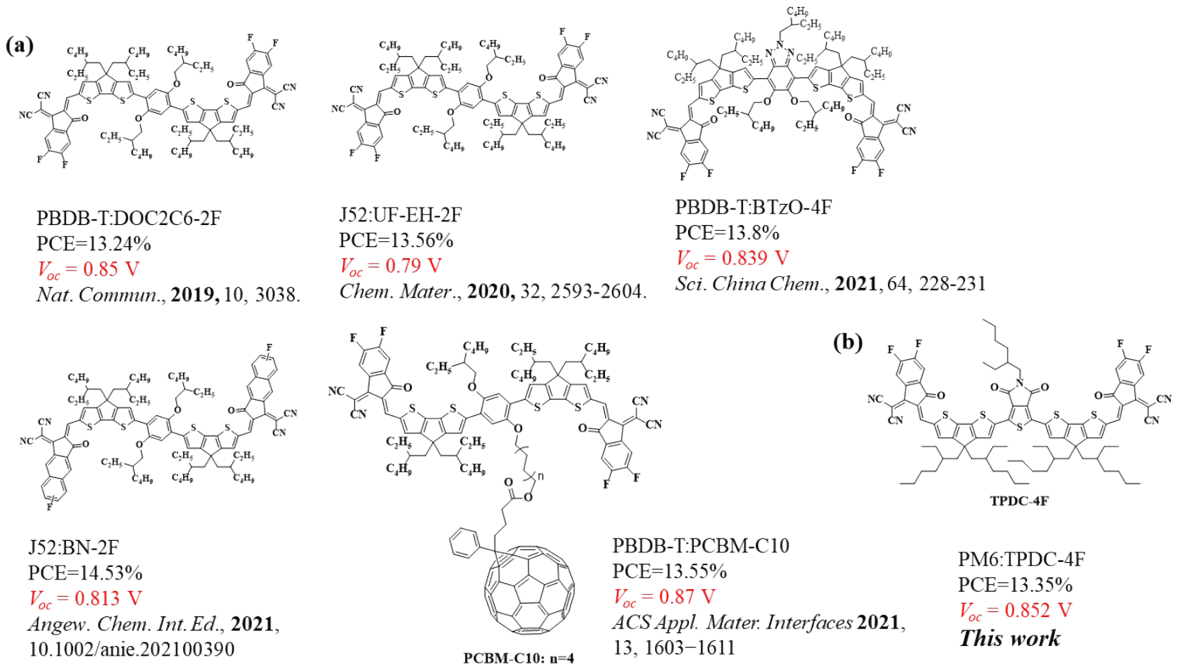

Fig. S20 (a) Chemical structure, power conversion efficiency (PCE over 13%) and open-circuit voltage of the representative high-performance organic solar cell based on non-fused ring electron acceptors in the literature. (b) Molecular structure of non-fused ring acceptor TPDC-4F reported in this work.

References

[1] C. Piliego, T. W. Holcombe, J. D. Douglas, C. H. Woo, P. M. Beaujuge, and J. M. J. Fréchet, *J. Am. Chem. Soc.*, 2010, **132**, 7595-7597.

[2] X. Guo, N. Zhou, S. J. Lou, J. W. Hennek, R. P. Ortiz, M. R. Butler, P. L. Boudreault, J. Strzalka, P. O. Morin, M. Leclerc, J. T. López Navarrete, M. A. Ratner, L. Chen, R. P. Chang, A. Facchetti and T. J. Marks, *J. Am. Chem. Soc.*, 2012, **134**, 18427-18439.

[3] J. Yao, B. Qiu, Z. G. Zhang, L. Xue, R. Wang, C. Zhang, S. Chen, Q. Zhou, C. Sun, C. Yang, M. Xiao, L. Meng and Y. Li, *Nat. Commun.*, 2020, **11**, 2726.

[4] Y. Sun, J. H. Seo, C. J. Takacs, J. Seifter and A. J. Heeger, *Adv. Mater.*, 2011, **23**, 1679-1683.

[5] G. G. Malliaras, J. R. Salem., P. J. Brock and C. Scott, *Phys. Rev. B.*, 1998, **58**, 13411.

[6] S. Li, L. Zhan, F. Liu, J. Ren, M. Shi, C.-Z. Li, T. P. Russell and H. Chen, *Adv. Mater.*, 2018, **30**, 1705208.

[7] N. Wang, L. Zhan, S. Li, M. Shi, T.-K. Lau, X. Lu, R. Shikler, C.-Z. Li and H. Chen, *Mater. Chem. Front.*, 2018, **2**, 2006-2012.

[8] S. Li, L. Zhan, W. Zhao, S. Zhang, B. Ali, Z. Fu, T.-K. Lau, X. Lu, M. Shi, C.-Z. Li, J. Hou and H. Chen, *J. Mater. Chem. A*, 2018, **6**, 12132-12141.

[9] R. Qin, W. Yang, S. Li, T.-K. Lau, Z. Yu, Z. Liu, M. Shi, X. Lu, C.-Z. Li and H. Chen, *Mater. Chem. Front.*, 2019, **3**, 513-519.

[10] S. Li, L. Zhan, C. Sun, H. Zhu, G.Zhou, W.ang, M. Shi, C.-Z. Li, J. Hou Y. Li and H. Chen, *J. Am. Chem. Soc.*, 2019, **141**, 3073-3082.

[11] S. Li, L. Zhan, T.-K. Lau, Z. P. Yu, W. Yang, T. R. Andersen, Z. Fu, C. Z. Li, X. Lu, M. Shi and H. Chen, *Small Methods*, 2019, **3**, 1900531.

[12] S. Pang, X. Zhou, S. Zhang, H. Tang, S. Dhakal, X. Gu, C. Duan, F. Huang and Y. Cao, *ACS Appl*. *Mater*. *Interfaces*, 2020, **12**, 16531-16540.

[13] Y.-Q.-Q. Yi, H. Feng, N. Zheng, X. Ke, B. Kan, M. Chang, Z. Xie, X. Wan, C. Li, and Y. Chen, *Chem. Mater.*, 2019, **31**, 3, 904-911.

[14] Y. Wang, Z. Wang, X. Cui, C. Wang, H. Lu, Y. Liu, Z. Fei, Z. Ma and Z. Bo, *J. Mater. Chem. A*, 2020, **8**, 12495-12501.

[15] C. He, Y. Li, S. Li, Z. P. Yu, Y. Li, X. Lu, M. Shi, C.-Z. Li and H. Chen, *ACS Appl. Mater. Interfaces*, 2020, **12**, 16700-16706.

[16] S. Geng, W. Yang, J. Gao, S. Li, M. Shi, T.-K. Lau, X. Lu, C.-Z. Li and H. Chen, *Chinese J. Polym. Sci.*, 2019, **37**, 1005-1014.

[17] C. Chen, X. Chen, K. K. Liu, M. Zhang, J. Qu, C. Yang, G. Z. Yuan, A. Mahmood, F. Liu, F. He, D. Baran and J. Wang, *Small*, 2020, **16**, 1907681.

[18] H. Huang, Q. Guo, S. Feng, C. Zhang, Z. Bi, W. Xue, J. Yang, J. Song, C. Li, X. Xu, Z. Tang, W. Ma and Z. Bo, *Nat. Commun.*, 2019, **10**, 3038.

[19] M. Chang, L. Meng, Y. Wang, X. Ke, Y.-Q.-Q. Yi, N. Zheng, W. Zheng, Z. Xie, M. Zhang, Y. Yi, H. Zhang, X. Wan, C. Li and Y. Chen, *Chem. Mater.*, 2020, **32**, 2593-2604.

[20] X. Liu, Y. Wei, X. Zhang, L. Qin, Z. Wei and H. Huang, *Sci. China Chem.*, 2021, **64**, 228-231.

[21] D. Luo, X. Lai, N. Zheng, C. Duan, Z. Wang, K. Wang and A. K. K. Kyaw, *Chem. Eng. J.*, 2021, **420**, 129768.

[22] J. Lee, S.-J. Ko, M. Seifrid, H. Lee, B. R. Luginbuhl, A. Karki, M. Ford, K. Rosenthal, K. Cho, T.-Q. Nguyen and G. C. Bazan, *Adv. Energy Mater.*, 2018, **8**, 1801212.

[23] J. Lee, S.-J. Ko, H. Lee, J. Huang, Z. Zhu, M. Seifrid, J. Vollbrecht, V. V. Brus, A. Karki, H. Wang, K. Cho, T.-Q. Nguyen and G. C. Bazan, *ACS Energy Lett.*, 2019, **4**, 1401-1409.

[24] Z.-P. Yu, Z-X. Liu, F.-X. Chen, R. Qin, T.-K. Lau, J.-L. Yin, X. Kong, X. Lu, M. Shi, C.-Z. Li and H. Chen, *Nat Commun.*, 2019, **10**, 2152.

[25] K. Wang, J. Lv, T. Duan, Z. Li, Q. Yang, J. Fu, W. Meng, T. Xu, Z. Xiao, Z. Kan, K. Sun and S. Lu, *ACS Appl. Mater. Interfaces*, 2019, 11, 6717-6723.

[26] Z. Kang, S.-C. Chen, Y. Ma, J. Wang and Q. Zheng, *ACS Appl. Mater. Interfaces*, 2017, **9**, 24771-24777.

[27] J. Jung and W. Jo, *Chem. Mater.*, 2015, **27**, 6038-6043.

[28] Y. Patil, R. Misra, M. L. Keshtovb and G. D. Sharma, *J. Mater. Chem. A*, 2017, **5**, 3311.

[29] M. Privado, V. Cuesta, P. Cruz, M. L. Keshtov, R. Singhal, G. D. Sharmad and F Langa, *ACS Appl. Mater. Interfaces*, 2017, **9**, 11739-11748.

[30] M. Privado, V. Cuesta, P. Cruz, M. L. Keshtov, G. D. Sharma and F Langa, *J. Mater. Chem. A.*, 2017, **5**, 14259-14269.

[31] M. Privado, P. Cruz, S. Biswas, R. Singhal, G. D. Sharma and F. Langa, *J. Mater. Chem. A*, 2018, **6**, 11714-11724.

[32] X. Zhang, L. Qin, J. Yu, Y. Li, Y. Wei, X. Liu, X. Lu, F. Gao and H. Huang, *Angew. Chem. Int. Ed.*, 2021, **60**, 12475.

[33] Y. Zhou, M. Li, S. Shen, J. Wang, R. Zheng, H. Lu, Y. Liu, Z. Ma, J. Song and Z. Bo, *ACS Appl. Mater. Interfaces*, 2021, **13**, 1603-1611.